Microstructural and Mechanical Characterization of Ti-12Mo-6Zr Biomaterials Fabricated by Spark Plasma Sintering

WALID MOHAMED RASHAD MOHAMED DAOUSH, HEE SUP PARK, FAWAD INAM, BYUNG KYU LIM, and SOON HYUNG HONG

Ti-12Mo-6Zr/Al_2O_3 (titanium biomaterial) was prepared by a powder metallurgy route using Spark Plasma Sintering (SPS). Ti, Mo, and Zr powders were mixed by wet milling with different content of alumina nanoparticles (up to 5 wt pct) as an oxide dispersion strengthening phase. Composite powder mixtures were SPSed at 1273 K (1000 °C) followed by heat treatment and quenching. Composite powders, sintered materials, and heat-treated materials were examined using optical and high-resolution electronic microscopy (scanning and transmission) and X-ray diffraction to characterize particle size, surface morphology, and phase identifications for each composition. All sintered materials were evaluated by measuring density, Vickers hardness, and tensile properties. Fully dense sintered materials were produced by SPS and mechanical properties were found to be improved by subsequent heat treatment. The tensile properties as well as the hardness were increased by increasing the content of Al_2O_3 nanoparticles in the Ti-12Mo-6Zr matrix.

DOI: 10.1007/s11661-014-2693-3

I. INTRODUCTION

CURRENTLY, the most commonly used materials in biomedical applications are metals, ceramics, polymers, and composites. Because prosthetic devices and components need to fulfill several imperative requirements, they need to remain integral over a long use period without being rejected by the human body. The design and selection of biomaterials depend on the type of medical application. Materials used as implants are expected to be non-toxic and should not cause any inflammatory or allergic reactions to the human organs.[1–3] It is well known that all metals and alloys are subjected to corrosion when in contact with bodily fluid. A variety of chemical reactions can occur on the surface of a surgically implanted alloy. On the other hand, the mechanical properties decide the type of material that can be selected for a specific application. Some of the mechanical properties for bio applications that are of prime importance are hardness, fatigue life, tensile strength, modulus, and elongation.[4–7]

Materials generally used currently for surgical implants are 316L stainless steel, cobalt chromium (Co-Cr) alloys, and titanium and its alloys. Elements such as Ni, Cr, and Co are found to be leached from the stainless steel and cobalt chromium alloys due to corrosion in the body environment.[8,9] Skin-related diseases, such as dermatitis due to Ni toxicity, have been reported and numerous animal studies have shown carcinogenicity due to the presence of Co.[10] In addition, both 316L stainless steel and Cr-Co alloys possess much higher modulus than bone, leading to insufficient stress transfer to bone, which causes bone resorption and loosening of implant after some years of implantation.[11] Among the materials available for implant applications, the natural selection of titanium-based materials for implantation is due to the combination of its outstanding characteristics such as high strength, low density, good corrosion resistance, good biocompatibility, low modulus, and high capacity to join with bone and other tissues.[12,13] Commercially available pure Ti and Ti-6Al-4V are the most commonly used titanium materials for implant applications.

Ti-6Al-4V alloys are currently widely used as a candidate material for various bio applications due to their superior mechanical properties. Aluminum is added to stabilize the alpha phase and vanadium is added to stabilize the beta phase. Although titanium is a biocompatible metal, aluminum and vanadium have some detrimental toxicological effects on human body. Recent trends in titanium alloy development for biomedical applications include replacing vanadium by other elements such as Nb, Ta, and Mo for stabilizing the beta phase, whereas Zr and Hf are added for

WALID MOHAMED RASHAD MOHAMED DAOUSH, Associate Professor and Department Head, is with the Department of Production Technology, Faculty of Industrial Education, Helwan University, 30 El Sawah Street, Cairo 11511-11668, Egypt. Contact e-mail: waliddaoush@techedu.helwan.edu.eg HEE SUP PARK, Researcher, is with the Institute of Industrial Technology, ILJIN Diamond Co., Ltd., 614-2 Oryu-Ri, Daeso-Myun, Eumsung-Kun, Chungcheongbuk-Do 369-824, Republic of Korea. FAWAD INAM, Director of Mechanical Engineering, is with the Department of Mechanical and Construction Engineering, Faculty of Engineering and Environment, Northumbria University, Newcastle upon Tyne NE1 8ST, U.K. BYUNG KYU LIM, Researcher, and SOON HYUNG HONG, Professor and Head of the Composite Materials Lab. are with the Composite Materials Lab., Department of Materials Science and Engineering, Korea Advanced Institute of Science and Technology, 291 Daehak-ro, Yuseong-gu, Daejeon 305-701, Republic of Korea.

Manuscript submitted April 21, 2014.
Article published online December 12, 2014

increasing the strength of the materials by stabilizing the alpha phase.[14–19] In an another report, Gibbesch *et al.*[20] added biocompatible additives to the pure alloys such as silicon carbide and alumina particles as a dispersed phase to increase the strength and other key mechanical properties.

Ceramics, as inorganic non-metallic materials, are among the few which can fulfill the requirements necessitated for orthopedic implants. Some ceramics exhibit good biocompatibility and mechanical strength, which makes them an alternative for heavily loaded prostheses. Furthermore, characteristics such as high hardness, which generally means high wear and scratch resistance, and good wettability especially by polar liquids such as synovial fluid, make ceramics desirable for bearing surface and tribological applications.[21–23] Other important properties of ceramics are chemical stability, corrosion resistance, and insolubility in water, which avoid degradation of the material and allergic reactions in the human body. For these reasons, ceramic materials have been found to be very useful for applications like bearing surfaces. Alumina, zirconia, and its composites are the commonly used ceramics for bearing applications.[24,25]

Alumina possesses high hardness, good stability, high oxidization capability, very low coefficient of friction (high wear resistance), low bending stress, and good biocompatibility.[26–28] The first clinical use of alumina was in 1970 for total hip prostheses.[29] It was expected that alumina would provide more stable cementless fixation due to its good biocompatibility and as a result, alumina ceramics for knee replacements were also investigated.[30–34] A major concern with alumina ceramics is high rigidity (*i.e.*, elastic modulus of about 350 GPa) that is responsible for stress protection and aseptic loosening.[35] Furthermore, alumina is not bioactive and provides no direct bone/material interface leading to micromotion. Although alumina has many advantages as a compatible biomaterial, it should be noted that it possesses relatively low fracture toughness. Its fracture toughness is lower than that of the metallic materials used in orthopedic applications, thus it is very brittle and shows no deformation until breakage.[32] However, some of the recent research[36] has reported good mechanical properties for alumina ceramics.

Over the past few years, adding nanoparticles for improving corrosion resistance of biomaterials is receiving significant research attention. The technology is largely used for introducing of organic or inorganic nanoparticles on the surface of substrate.[37,38] Nanoparticles also enhance chances of selective oxidation which forms tenacious oxide on the surface of biomaterial, such as nanophase titania, alumina, and hydroxyapatite.[39–44]

In the present work, authors replace vanadium by molybdenum as a low-toxic beta stabilizer and zirconium instead of aluminum to stabilize the alpha phase. Such substitution was carried out to increase the tensile properties of the produced biomaterial as well. In addition, the paper analyzes the effect of addition of alumina nanoparticles (oxide dispersion strengthen phase) on the mechanical properties of the sintered biomaterial. Ti-12Mo-6Zr/Al_2O_3 biomaterials with different alumina nanoparticles content up to 5 wt pct were prepared by conventional mixing of its powder constituents followed by SPS and heat treatment.

II. MATERIALS

Titanium powder of 50 μm particle size (Starmet Co.), molybdenum powder of 5 μm particle size (Aldrich Co. LTD), zirconium of 3 μm particle size (SE-Jong Materials LTD), and alumina nanoparticles of 300 nm powder (Sumitomo chemical Co.) were used as powder constituents for preparing Ti-12Mo-6Zr/Al_2O_3 biomaterials. Different alumina concentrations of 0, 1, 2.5, and 5 wt pct were used. Figures 1(a) through (d) show SEM images of the powders.

III. METHODS

Mixtures were prepared by wet milling of the powder constituents in ethanol using alumina balls of 5 mm diameter. The milling conditions were: milling speed of 40 RPM for 48 hours and the ratio of powder, balls, and ethanol were 1:1:1 by weight.

Milled powders were dried under vacuum for 2 hours at 353 K (80 °C) for complete evaporation of ethanol. All powder mixtures were SPSed using Dr. SINTER.LAB apparatus. SPS enables fabrication of fully sintered product using joule heat generated by high-pulsed electric current applied through the compact and is widely used for fabricating microstructures that cannot be produced by any other method.[45] A 15-mm-diameter uniaxial graphite die was used to produce a 5-mm-thick sample for each composition. Optimum sintering conditions of 1273 K (1000 °C) for 5 minutes under 50 MPa were found. During SPS, heating rate of 100 K/min and 10^{-3} torr vacuum conditions were maintained for all samples. All sintered samples were heat treated at 1473 K (1200°C) for 6 hours under argon atmosphere followed by water quenching. Ti-12Mo-6Zr/Al_2O_3 sintered samples were ground using 800, 1200, 2000, and 4000 grade SiC papers, respectively. The ground samples were polished with 3 micron diamond paste. The microstructures were analyzed by field emission scanning electron microscopy of the Model XL30SFEG, and high-resolution transmission electron microscopy (JEM-3010), using an accelerating voltage of 300 kV. The phase compositions of the obtained sintered samples were identified using X-ray diffractometry (Rigaku D/MAX IIIC).

The sintered densities of the SPSed, as well as the heat-treated samples were measured by Archimedes density measurement according to MPIF standard 42 (1998). Hardness characterizations were conducted using Vickers microhardness tester (Mitutoyo) with an applied load of 2 kgf. At least 5 indentations were made for each sample. Tensile tests were performed using an Instron tensile testing machine (model 4206) and a crosshead speed of 0.2 mm/min. Dog-bone shaped subsize specimens were prepared by a wire cutting machine. A strain gage of the length of 9 mm and width of

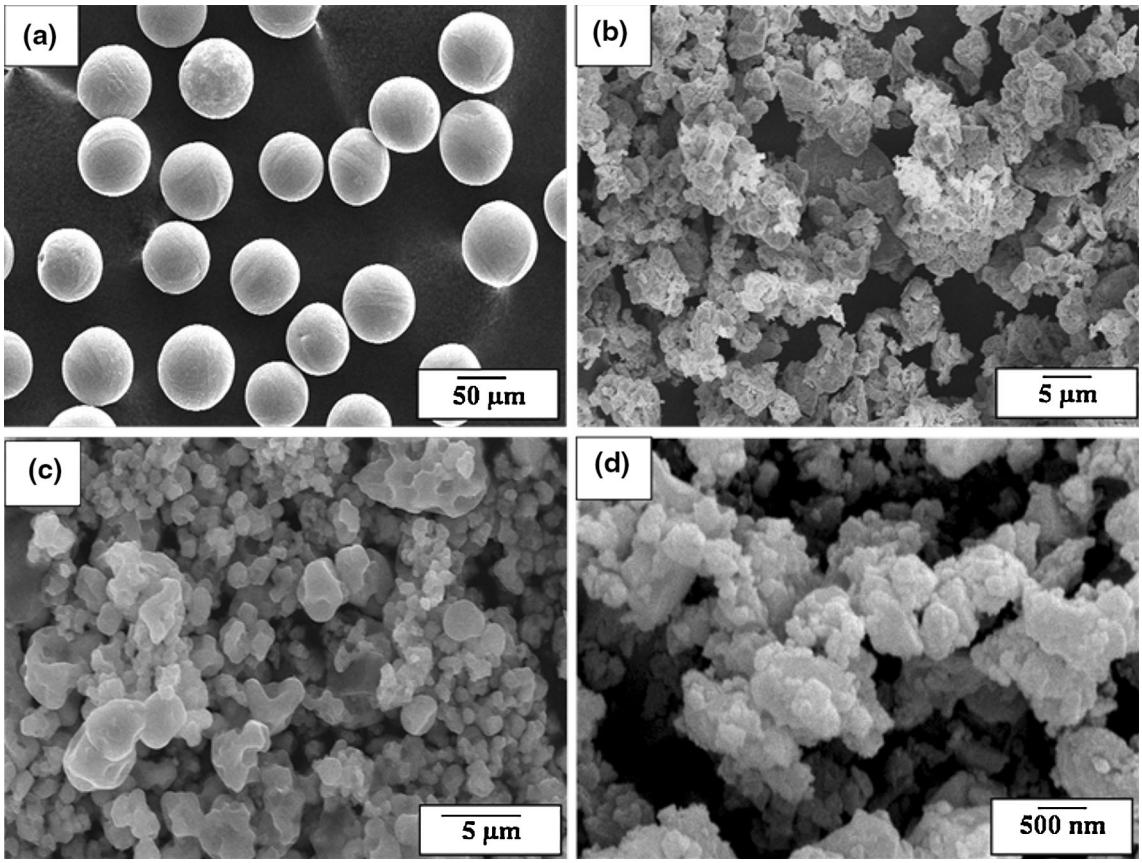

Fig. 1—SEM micrographs for the investigated powders were (*a*) titanium, (*b*) molybdenum, (*c*) zirconium, and (*d*) alumina nanoparticles.

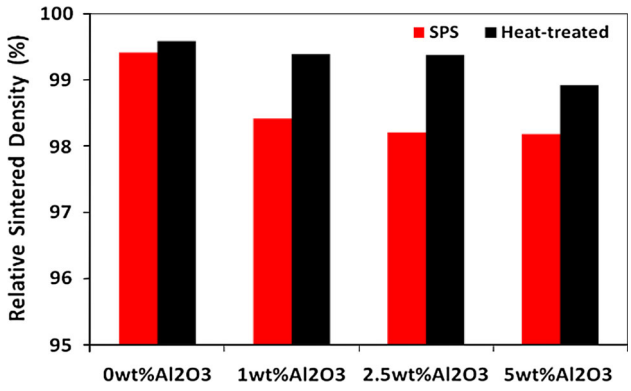

Fig. 2—The relative densities of the obtained Ti-12Mo-6Zr/Al_2O_3 sintered materials by spark plasma sintering and the heat-treated processes.

2.5 mm based on the ASTM E8M were used for tensile testing.

IV. RESULTS AND DISCUSSION

A. *Spark Plasma Sintering*

Preliminary studies were conducted over range of temperatures, times, and compaction pressures to determine optimal SPSing conditions. Shrinkage for all the samples stopped after 5 minutes of processing when the compaction pressure of 50 MPa at 1273 K (1000 °C) was maintained. Figure 2 shows the density values for the SPSed as well as heat-treated Ti-12Mo-6Zr/Al_2O_3 biomaterials with different Al_2O_3 concentrations. It was observed that Ti-12Mo-6Zr without any alumina achieved relatively higher densities of 99.4 pct. The density of Ti-12Mo-6Zr was decreased by increasing the amount of Al_2O_3. For instance, 1 wt pct Ti-12Mo-6Zr/Al_2O_3 was found to be 98.4 pct dense and it decreased slightly to 98.2 pct for 2.5 wt pct Ti-12Mo-6Zr/Al_2O_3 and to 98.2 for 5 wt pct Ti-12Mo-6Zr/Al_2O_3. The inclusion of Al_2O_3 nanoparticles in the matrix increased the porosity level subsequently decreasing the density of the material. Also, the densities of the SPSed compacts were increased after heat treatment. The heat treatment process is responsible for increasing the diffusion of the constituents which decreased porosity levels in the sintered materials.

B. *Microstructure Investigations of the Ti-12Mo-6Zr/Al_2O_3 Biomaterials*

Figure 3 shows SEM micrographs of the obtained Ti-12Mo-6Zr/Al_2O_3 sintered material. Al_2O_3 particles were found homogeneously distributed in the metal matrix with low Al_2O_3-Al_2O_3 particles interaction and low

porosity. In addition, the micrographs also show that the sintered materials have good bonding between the Al_2O_3 particles and metal matrix with low-porosity contents. The reason for the improved bonding and density of the sintered materials is mainly due to the diffusion of the aluminum from the alumina particles to the metal matrix as can be seen from the EDAX analysis of the matrix which indicated a small peak of aluminum (see Figures 3(e) and (f)).

Figure 4(a) shows XRD pattern of the raw powder mixtures. Four representative peaks were detected for the constituents (Ti, Mo, Zr, and alumina) of the prepared Ti-12Mo-6Zr/Al_2O_3 materials. For processed materials, two different intensive peaks in addition to low intensive peaks of alumina particles were detected for the SPSed as well as the heat-treated materials. Those intensive peaks were of α and β phases. The α/β phase transformation is influenced by the heat treatment

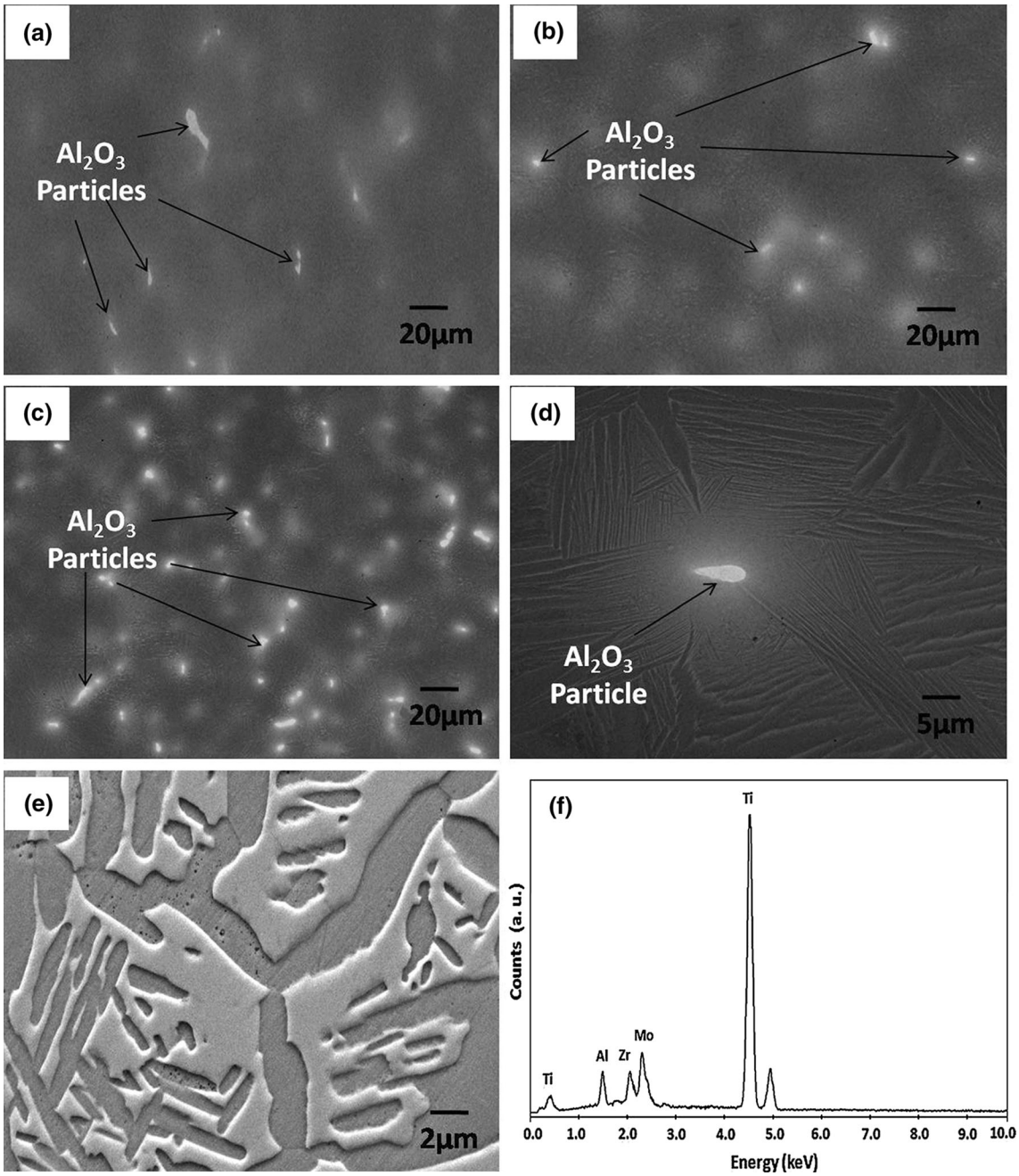

Fig. 3—SEM micrographs for the obtained sintered materials were (*a*) 1 wt pct Ti-12Mo-6Zr/Al_2O_3, (*b*) 2.5 wt pct Ti-12Mo-6Zr/Al_2O_3, (*c*) and (*d*) low and high magnification images of 5 wt pct Ti-12Mo-6Zr/Al_2O_3, (*e*) and (*f*) is the SEM/EDAX analysis of the 5 wt pct Ti-12Mo-6Zr/Al_2O_3 matrix.

process as shown in Figures 3(b) and (c). As expected, this is due to the water quenching of the heat-treated samples that changed the α/β phase ratios. Microstructures go through a series of changes during heat treatment. Microstructure observations revealed marked changes of α particle size during heat treatment. After heat treatment, α particle thickness was increased. There was no doubt that the dimensions and quantity of α particle continued to increase during heat treatment. It is commonly known that higher heat treatment temperatures are more favorable for static coarsening behavior.[46]

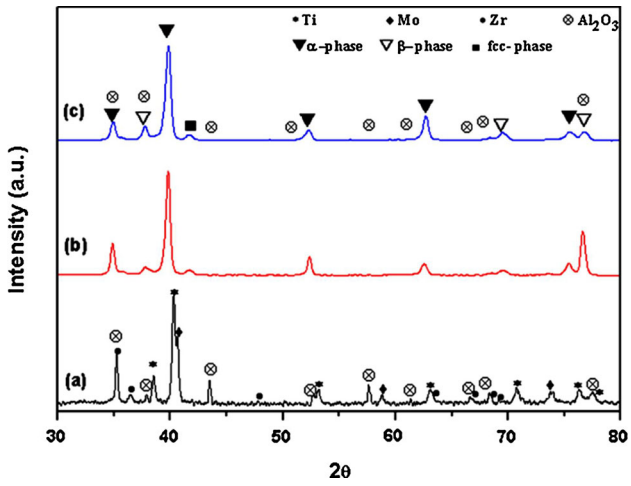

Fig. 4—XRD patterns for (*a*) as mixed Ti, Mo, Zr, and 5 wt pct Al_2O_3 powders (*b*) as sintered 5 wt pct Ti-12Mo-6Zr/Al_2O_3 and (*c*) heat-treated 5 wt pct Ti-12Mo-6Zr/Al_2O_3 materials.

Figures 5(a) to (d) show high magnification SEM images of the α/β lamellar structure for the SPSed Ti-12Mo-6Zr/Al_2O_3 with different content of Al_2O_3. By increasing the Al_2O_3 content, a thick needle-like α phase was found precipitating in the matrix. It was observed that by increasing the Al_2O_3 content from 0 to 5 wt pct, the α needle phase in the α/β lamellar structure becomes courser and the orientation of the needles changes from unidirectional to multidirectional. This is due to the diffusion of the aluminum from alumina to the matrix, which is increased by increasing the amount of the reinforced alumina particles in the metal matrix Al.[47]

Figure 6(a) shows high-resolution TEM image of the Ti-12Mo-6Zr/Al_2O_3 sintered material. The microstructure shows several nanoparticles precipitated in the matrix. From the EDAX semi-quantitative analysis of these particles, intermetallic compounds of Ti, Mo, Zr, and Al metals were found (Figure 6(b)). These intermetallic compounds were formed due to the interactions

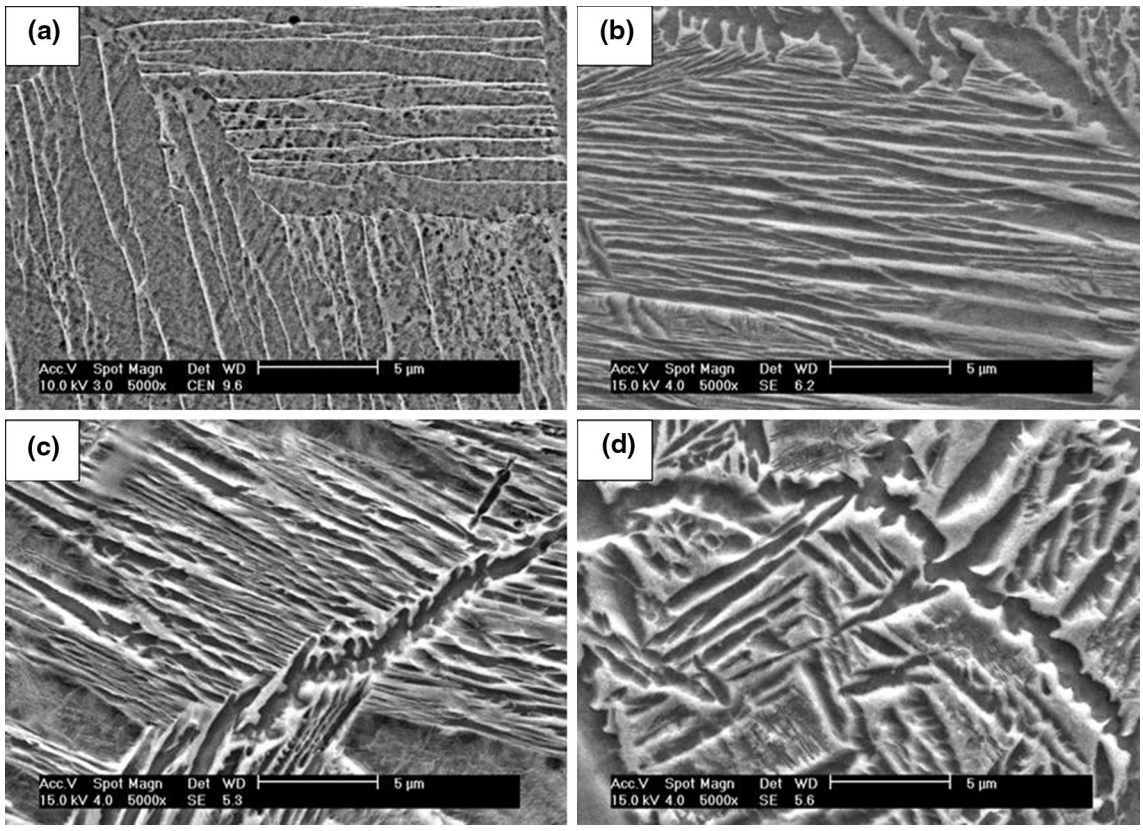

Fig. 5—SEM micrographs for the sintered materials were (*a*) Ti-12Mo-6Zr, (*b*) 1 wt pct Ti-12Mo-6Zr/Al_2O_3, (*c*) 2.5 wt pct Ti-12Mo-6Zr/Al_2O_3, and (*d*) 5 wt pct Ti-12Mo-6Zr/Al_2O_3 materials.

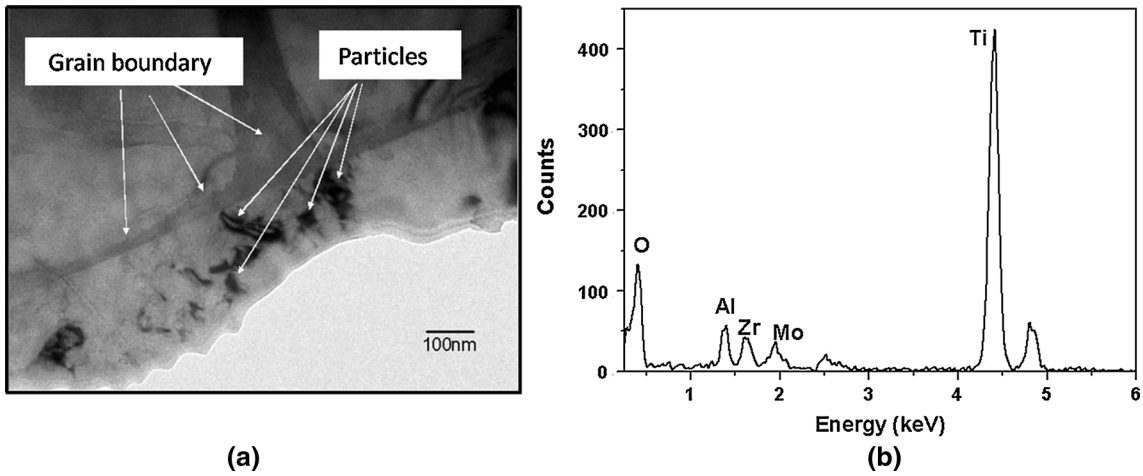

Fig. 6—(*a*) TEM micrograph and (*b*) EDS semi-quantitative analysis for the dispersed oxide particles in the matrix of heat-treated 2.5 wt pct Ti-12Mo-6Zr/Al_2O_3 material.

between the alumina nanoparticles and the constituents of the Ti-12Mo-6Zr metal matrix.

C. *Mechanical Properties*

Figure 7 shows the effect of the alumina wt pct on the hardness of Ti-12Mo-6Zr/Al_2O_3 materials. It was observed that by increasing the alumina content up to 5 wt pct, the hardness was increased to 575 HV. This is due to the contribution of the hard alumina nanoparticles in the metal matrix. In addition, the interaction between the reactive metals (Ti, Mo, and Zr) and the alumina nanoparticles enhanced the formation of the intermetallics nanoparticles, as observed in Figure 6(a), which also increased the hardness values. Similarly, heat-treated samples have higher hardness as compared to SPSed materials. It is due to the increase in the density and decrease in the porosity of the heat-treated samples. This subsequently increased the hardness.

The measured Young's moduli of the Ti-12Mo-6Zr/Al_2O_3 sintered materials are plotted in Figure 8 as a function of the alumina content. It can be seen that the Young's modulus of Ti-12Mo-6Zr/Al_2O_3 sintered material increased by increasing the alumina content. The Young's modulus increased from 50 GPa (pure Ti-12Mo-6Zr) to a maximum value of 280 GPa (5 wt pct Ti-12Mo-6Zr/Al_2O_3). Young's modulus, which is an intrinsic material property, depends on atomic bonding.[48–52] It is related to the crystal structure and interatomic spacing and can be affected by alloying addition, heat treatment, and plastic deformation.[48–52] Since the conducted heat treatments were consistent for all materials and the Young's modulus is not sensitive to the grain size and morphology of materials,[53,54] the differences in elastic moduli between the studied materials is due to the differences in the chemical compositions (*i.e.*, alumina content).

The effect of alumina on the tensile properties of Ti-12Mo-6Zr/Al_2O_3 sintered materials is shown in Figure 8. Since the yield strength shows similar trend to the Young's modulus, it can be observed that the

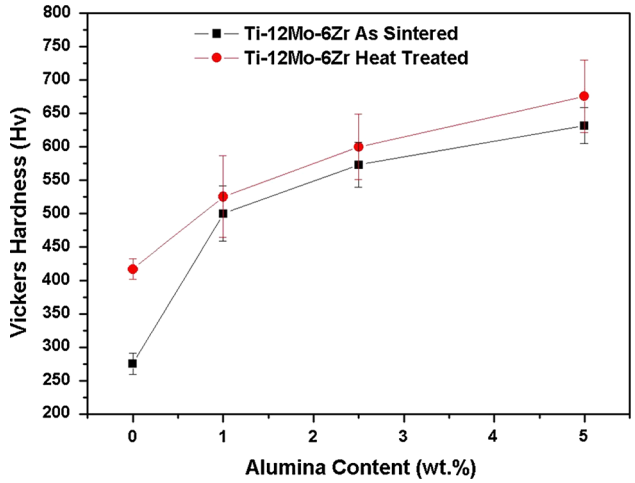

Fig. 7—Effect of alumina content on hardness of spark plasma sintered and heat-treated Ti-12Mo-6Zr/Al_2O_3 materials.

tensile strength of pure Ti-12Mo-6Zr sintered material is 310 MPa, and gradually increased with increasing alumina content up to 5 wt pct, reaching 455 MPa.

It was observed from the analysis of tensile properties (Figure 8) that there is a strong relation between the change in the strength and the microstructure. The variation in the strength of the Ti-12Mo-6Zr/Al_2O_3 sintered materials is due to the changes in microstructure caused by the interaction between the alumina nanoparticles and the reactive metals of the Ti-12Mo-6Zr matrix (Figure 9). The phenomenon of solid solution strengthening for sintered materials observed here became significant with the increase in alumina wt pct. Therefore, the increase in tensile strength is due to the increase in the α phase (Figure 5). The increase in the tensile properties of Ti-12Mo-6Zr/Al_2O_3 materials is related to its lamellar structures (Figure 5) as well (*i.e.*, occurrence of the needle phase). It was also observed that the elongation decreased by increasing the alumina wt pct from 7 pct (*i.e.*, for Ti-12Mo-6Zr) to 0.75 pct for

5 wt pct Ti-12Mo-6Zr/Al_2O_3. This is also consistent with the general assumption of the correlation between strength and ductility, *i.e.*, yield strength is inversely proportional to the ductility.[17,18]

The fractured surfaces were examined by SEM microscopy, and representative images are shown in Figures 8(a) and (b). It was observed that the sample with composition of Ti-12Mo-6Zr exhibits a transgranular cleavage (Figure 9(a)). The sample with composition of 5 wt pct Ti-12Mo-6Zr/Al_2O_3 exhibits a transgranular cleavage with finer grain size than the Ti-12Mo-6Zr (Figure 8(b)). From the analysis of the fractured surfaces of 5 wt pct Ti-12Mo-6Zr/Al_2O_3 sintered materials, it was also observed that there were particles at the grain boundaries (Figure 8(b)). These particles are alumina or intermetallics particles resulted from the interaction between the alumina particles and the reactive elements (Ti, Mo, and Zr) as shown in the EDAX semi-quantitative analysis (Figure 6(b)).

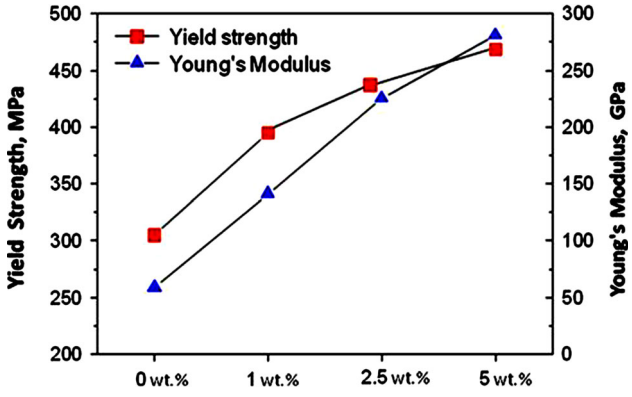

Fig. 8—Effect of alumina content on yield strength and elastic modulus of the sintered and heat-treated Ti-12Ta-6Zr materials.

V. CONCLUSIONS

The current study investigated the effect of alumina addition on the mechanical properties of Ti-12-Mo-6Zr biomaterials. The change in mechanical properties of the Ti-12Mo-6Zr and Ti-12Mo-6Zr/Al_2O_3 biomaterials was analyzed by investigating corresponding microstructures. By means of SPSing followed by heat treatment, sintered materials of lamellar microstructure with width up to 5 μm were obtained. The thickness of the lamellar structure increased with the increase in alumina content. The addition of alumina influenced hardness, yield strength, and Young's modulus of Ti-12Mo-6Zr and Ti-12Mo-6Zr/Al_2O_3 materials. Hardness, yield strength, and Young's modulus were increased by increasing the alumina content up to 5 wt pct.

The microstructure of the heat-treated sintered materials consists mainly of α or β phase with different morphologies. The presence of high amount of α lamellar and thicker phase in the microstructure increased hardness and tensile strength whereas the presence of β phases lowered these mechanical properties. By increasing the content of alumina particles, the hardness of the SPSed materials increased from 275 to 625 Hv. The hardness values were further increased between 410 and 675 Hv by heat treatment of the SPSed samples. It can now be concluded that the strengthening

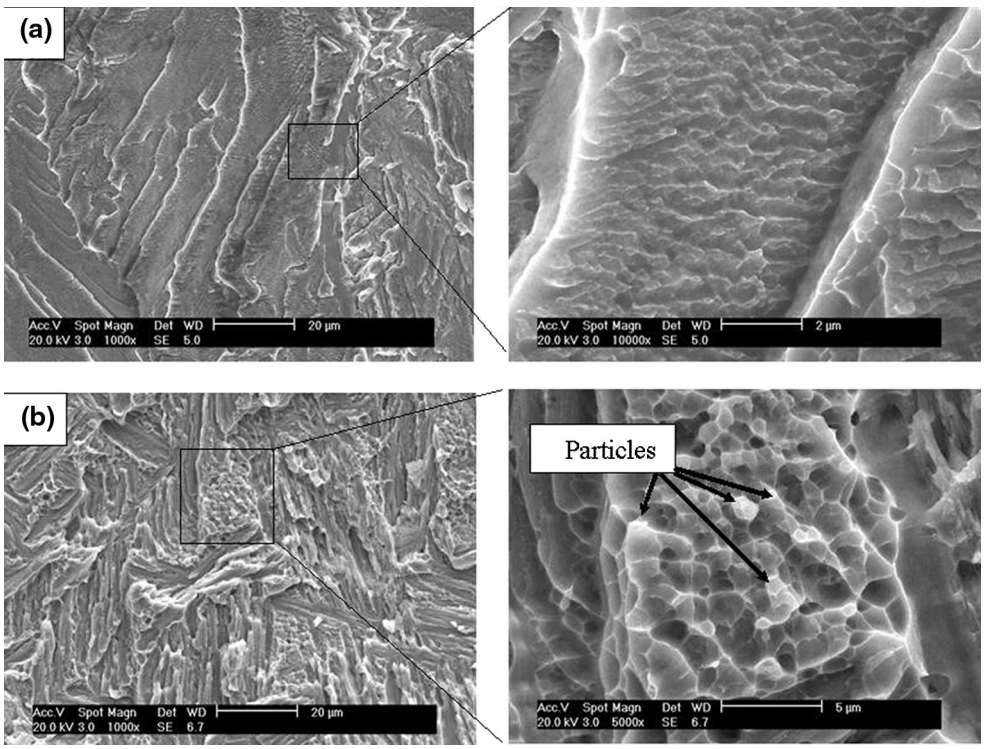

Fig. 9—SEM micrographs for the fracture surfaces of (*a*) Ti-12Mo-6Zr and (*b*) 2.5 wt pct Ti-12Mo-6Zr/Al_2O_3 sintered materials.

mechanisms of the obtained sintered materials is due to four reasons: (a) the dispersion of alumina particles in the metal matrix; (b) due to the formation of solid solution between aluminum from the alumina phase and the metal matrix; (c) microstructural coarsening and the formation of the α needle phase structure; and (d) the formation of the nanostructured intermetallic phases. The elastic modulus of the sintered materials was found in the range of 50 to 275 GPa, which is significantly lower than that of conventionally used stainless steel (210 GPa), Co-Cr alloys (204 to 240 GPa), and $\alpha + \beta$ titanium alloys (100 to 120 GPa) which all exhibit good combination of mechanical properties (elastic modulus 50 to 275 GPa and yield strength 310 to 455 MPa). Considering these properties, Ti-12Mo-6Zr and the related Ti-12Mo-6Zr/Al_2O_3 sintered materials possess significant potential for future biomedical load bearing applications.

ACKNOWLEDGMENT

The authors would like to acknowledge Prof. Randall M. German, professor of powder metallurgy at San Diego State University, for his guidance during the microstructural investigations and mechanical characterizations.

REFERENCES

1. Y.L. Zhou, M. Niinomi, and T. Akahori: *Mater. Sci. Eng. A*, 2004, vol. 384, pp. 92–101.
2. D.F. Williams: *Biomaterials*, 2008, vol. 29, pp. 2941–53.
3. Y.L. Zhou, M. Niinomi, and T. Akahori: *Mater. Sci. Eng. A*, 2004, vol. 371, pp. 283–90.
4. J.A. Davidson and F.S. Georgette: *Proceedings of the Implant Manufacturing and Material Technology*, Society of Manufacturing Engineers, Dearborn, 1987, pp. 122–26.
5. M. Niinomi: *Mater. Sci. Eng. A*, 1998, vol. 243, pp. 231–36.
6. K. Lawrence: *Nature*, 1980, vol. 283, pp. 106–07.
7. J. Black and G.W. Hastings: in *Handbook of Biomaterial Properties*, J. Black and G.W. Hastings, eds., Chapman & Hall, London, 1998.
8. O. Yoshimitsu, G. Emiko, and M. Takeshi: *Biomaterials*, 2004, vol. 25, pp. 5913–20.
9. K.L. Wapner: *Clin. Orthop. Relat. Res.*, 1991, vol. 271, pp. 12–20.
10. D.B. McGregor, R.A. Baan, C. Partensky, J.M. Rice, and J.D. Wilbourn: *Eur. J. Cancer*, 2000, vol. 36 (3), pp. 307–13.
11. S.H. Teoh: *Int. J. Fatigue*, 2000, vol. 22 (10), pp. 825–37.
12. M. Niinomi: *Metall. Mater. Trans. A*, 2001, vol. 33A, pp. 477–86.
13. M. Niinomi: *Sci. Technol. Adv. Mater.*, 2003, vol. 4, pp. 445–54.
14. D. Kuroda, M. Niinomi, M. Morinaga, Y. Kato, and T. Yashiro: *Mater. Sci. Eng. A*, 1998, vol. 243 (1–2), pp. 244–49.
15. M. Niinomi, D. Kuroda, K.I. Fukunaga, M. Morinaga, Y. Kato, T. Yashiro, and A. Suzuki: *Mater. Sci. Eng. A*, 1999, vol. 263, pp. 193–99.
16. D. Kuroda, M. Niinomi, H. Fukui, A. Suzuki, and S. Hasegawa:, in *Structural Biomaterials for the 21st Century*, M. Niinomi, T. Okabe, E.M. Taleff, D.R. Lesure, and H.E. Lippard, eds., TMS, Warrendale, 2001, pp. 99–106.
17. T. Akahori, M. Niinomi, T. Yabunaka, D. Kuroda, H. Fukui, A. Suzuki, and J. Hasegawa: in *Proceedings of the PRICM 4*, S. Hanada, Z. Zhong, S.W. Nam, and R.N. Wright, eds., The Japan Institute of Metals, Sendai, 2001, pp. 209–12.
18. S.G. Steinemann: in *Evaluation of Biomaterials*, G.D. Winter, J.L. Leray, and K. Grootde, eds., Wiley, New York, 1980, pp. 1–34.
19. H. Kawahara, S. Ochi, K. Tanetani, K. Kato, M. Isogai, Y. Mizuno, H. Yamamoto, and A. Yamaguchi: *J. Jpn. Soc. Dent. Apparat. Mater.*, 1963, vol. 4 (65), pp. 65–75.
20. B. Gibbesch, G. Elssner, and G. Petzow: *Int J Oral Maxillofac Implants*, 1989, vol. 4 (2), pp. 131–37.
21. B.S. Bal, J. Garino, M. Ries, and M.N. Rahaman: *Semin Arthroplasty*, 2006, vol. 17, pp. 94–101.
22. B.E. Bierbaum, J. Nairus, D. Kuesis, J.C. Morrison, and D. Ward: *Clin. Orthop. Relat. Res.*, 2002, vol. 405, pp. 158–63.
23. J.D. Chang, K. Billau, M.C. Lee, and J.W. Ahn: *Steinkopff*, 2007, pp. 123–32.
24. R.S. Laskin: *Tech. Knee Surg.*, 2004, vol. 3, pp. 187–92.
25. T. Pandorf and M. Kuntz: *Bioceram. Altern. Bear. Jt. Arthroplast.*, 2007, pp. 137–43.
26. H.B. Skinner: *Clin. Orthop. Relat. Res.*, 1999, pp. 83–91.
27. D. Hannouche, M. Hamadouche, R. Nizard, P. Bizot, A. Meunier, and L. Sedel: *Clin. Orthop. Relat. Res.*, 2005, vol. 430, pp. 62–71.
28. J. Harms and E. Mausle: *J. Biomed. Mater. Res.*, 1979, vol. 13, pp. 67–87.
29. P. Boutin: *La Presse Méd.*, 1971, vol. 79, pp. 639–640.
30. H. Oonishi, S. Kim, M. Kyomoto, M. Iwamoto, and M. Ueno: *Bioceram Altern Bear. Jt. Arthroplast.*, 2006, pp. 101–10.
31. M. Semlitsch, M. Lehmann, and H. Weber: *J. Biomed. Mater. Res.*, 1977, vol. 11, pp. 537–52.
32. H. Oonishi, H. Fujita, S. Itoh, S. Kin, H. Amino, and E. Tsuji: in *Key Engineering Materials*, S. Brown, I. Clarke, and P. Williams, eds., Palm Springs, CA, 2002, pp. 499–502.
33. H. Oonishi, H. Fujita, S. Itoh, S. Kin, and H. Amino: in *Key Engineering Materials*, S. Brown, I. Clarke, and P. Williams, eds., Palm Springs, CA, 2002, pp. 479–82.
34. H. Oonishi, L. Hench, J. Wilson, F. Sugihara, E. Tsuji, M. Matsuura, S. Kin, T. Yamamot, and S. Mizokawa: *J. Biomed. Mater. Res.*, 2000, vol. 51 (1), pp. 37–46.
35. P. Boutin, P. Christel, J.M. Dorlot, A. Meunier, A. De Roquancourt, D. Blanquaert, S. Herman, L. Sedel, and J. Witvoet: *J. Biomed. Mater. Res.*, 1988, vol. 22, pp. 1203–32.
36. T. Majima, K. Yasuda, H. Tago, Y. Aoki, and A. Minami: *Knee Surg. Sports Traumatol. Arthrosc.*, 2008, vol. 16, pp. 152–56.
37. G. Carbajal, A. Martinez-Villafane, J.G. Gonzalez-Rodriguez, and V.M. Castano: *Anti-Corros. Methods Mater.*, 2001, vol. 48, pp. 241–45.
38. G.X. Shen, Y.C. Chen, and C.J. Lin: *Thin Solid Films*, 2005, vol. 489, pp. 130–36.
39. T.J. Webster, C. Ergun, R.H. Doremus, R.W. Siegel, and R. Bizios: *Biomaterials*, 2000, vol. 21, pp. 1803–10.
40. T.J. Webster, R.W. Siegel, and R. Bizios: *Biomaterials*, 1999, vol. 20, pp. 1222–27.
41. A. Bigi, N. Nicoli-Aldini, and B. Bracci: *J. Biomed. Mater. Res. A*, 2007, vol. 82, pp. 213–21.
42. M. Sato, A. Aslani, M.A. Sambito, N.M. Kalkhoran, E.B. Slamovich, and T.J. Webster: *J. Biomed. Mater. Res. A*, 2008, vol. 84, pp. 265–72.
43. Y. Wang, S. Lim, J.L. Luo, and Z.H. Xu: *Wear*, 2006, vol. 260, pp. 976–83.
44. Y.M. Wang, L.X. Guo, J.H. Ouyang, Y. Zhou, and D.C. Jia: *Appl. Surf. Sci.*, 2009, vol. 255, pp. 6875–80.
45. H.F. Jackson, D.D. Jayaseelan, M.J. Reece, F. Inam, D. Manara, C.P. Casoni, F. De Bruycker, K. Boboridis, and W.E. Lee: *Int. J. Appl. Ceram. Technol.*, 2010, vol. 7, pp. 316–26.
46. J. Xu, W. Zeng, Z. Jia, X. Sun, and J. Zhou: *J. Alloy. Compd.*, 2015, vol. 618, pp. 343–48.
47. H.N. Lee, D.R. Johnson, H. Inui, M.H. Oh, D.M. Wee, and M. Yamaguchi: *Acta Mater.*, 2000, vol. 48 (12), pp. 3221–33.
48. Y.L. Hao, M. Niinomi, D. Kuroda, K. Fukunaga, Y.L. Zhou, R. Yang, and A. Suzuki: *Metall. Mater. Trans. A*, 2002, vol. 33A, pp. 3137–44.
49. Y.T. Lee, M. Peters, and G. Welsch: *Metall. Trans. A*, 1991, vol. 22A, pp. 709–14.
50. Z.X. Cui: *Metallography and Heat Treatments*, Mechanical Industry Press of China, Beijing, 2000.
51. D.E. Dieter: *Mechanical Metallurgy*, 2nd ed., McGraw-Hill Ltd., Tokyo, 1976.

52. D.J. Mack: *Trans. AIME*, 1946, vol. 166, pp. 68–85.
53. S. Li, Y. Hao, R. Yang, Y. Cui, and M. Niinomi: *Mater. Trans.*, 2002, vol. 43 (12), pp. 2964–69.
54. Y. Song, R. Yang, Z.X. Guo, and D. Li: in *Structural Biomaterials for 21st Century*, M. Niinomi and H. Rack, eds., TMS, Warrendale, PA, 2001, pp. 273–80.